

On MIMO Relay with Finite-Rate Feedback and Imperfect Channel Estimation

Abstract—We investigate how finite-rate feedback and imperfect channel estimation impact MIMO relay network throughput and design in this paper. We start from multi-antenna transceiver with random beamforming and formulate the SNR and capacity loss due to channel estimation and quantization errors. We thereafter extend the analysis to multi-antenna relay network with multiple MIMO relay hops and discuss how the end-to-end throughput is scaled by MIMO pilot size, codebook size, relay network size and inter-beam interference. Some tradeoffs for MIMO relay network design are revealed. Computer simulations are provided to demonstrate our results.

I. INTRODUCTION

Multi-antenna systems have received much attention over the last decades, due to their promise of higher spectrum efficiency with no transmit power increase. Combining multi-antenna transceiver with relay network is essential not only to provide comprehensive coverage but also to help relieve co-channel interference in existing wireless systems. For multiple-input multiple-output (MIMO) transmission, it is well-known that their performance and complexity can be improved by making channel state information (CSI) available at the transmitter side. This is usually achieved through a reverselink CSI feedback channel from receiver, e.g., there is R-CQI channel for CSI feedback in UMB (Ultra Mobile Broadband), a 3.5G mobile network standard developed by 3GPP2. In practice, the CSI received by the transmitter is not perfect and suffers from various impairments and limitations that include round-trip delay, channel estimation error, codebook limitation, etc. Therefore the actual link throughput is degraded. This kind of degradation becomes more serious if the end-to-end capacity is considered for a multi-hop MIMO relay network.

MIMO beamforming with quantized feedback has intensively been investigated since 1990s [1]. MIMO channel quantization as well as codebook design in general is a NP-hard Voronoi decomposition problem. The Voronoi region for a uniform random codebook is known to be upper-bounded by the disk-covering problem solution and lower-bounded by the sphere-packing problem solution. These two bounds are open problems too. MISO/MIMO beamforming systems with perfect CQI Lloyd vector quantization (VQ) [2], different channel model [3] or different performance metrics [4], [5] have intensively been investigated. It is linked to Grassmannian packing problem [6]. However, most of existing work is done without considering pilot design and channel estimation, even though they are among the most important components of actual multi-antenna systems. In reality, MIMO CSI is estimated with forwardlink pilot channels from each antenna. An overview of pilot-assisted transmission (PAT)

including pilot design and channel estimation can be found in [7]. Pilot channels are usually designed to be orthogonal to other channels. Nonorthogonal pilot design like superimposed pilots (SIP) has recently received much attention for channel estimation too [8]. In practical system design, it is important to understand how MIMO pilot pattern and codebook design affect system throughput, what are the tradeoffs between them, etc. And these problems become more critical when a multi-hop MIMO relay network with beamforming is considered.

It is known that there is no simple solution to optimal MIMO channel quantization and codebook design. In this paper, a heuristic Voronoi boundary, *Hamming boundary*, is presented with the concept of Hamming bound. This heuristic boundary can be taken as a tradeoff between disk-covering circle (or hypercircle) and sphere-packing polytope and they all asymptotically converge when the codebook size is large. With this Hamming boundary, the MIMO beamforming signal-to-interference/noise ratio (SINR) with channel quantization is formulated and discussed. Besides this, *Cramer-Rao lower bound* (CRLB) on MIMO channel estimation with time-multiplexed pilots (TMP) or SIP is presented and analyzed. It is shown that channel estimation error affects the accuracy of both MIMO beamforming precoding and beam power allocation. We then extend our work to MIMO relay network and discuss the scalability of MIMO relay throughput by codebook size, pilot size, relay network size, etc. We show that MIMO relay network with imperfect CSI becomes interference-limited in high SNR region and it becomes more efficient to use more hops instead of increasing SNR for higher network throughput. This is different to the network operating in low interference region.

II. SYSTEM MODEL AND PROBLEM DESCRIPTION

Consider a MIMO link consisting of a transmitter with M transmit antennas, a receiver with N receive antenna and a MIMO channel represented by the $N \times M$ matrix $\mathbf{H} = [\mathbf{h}_1 \ \mathbf{h}_2 \ \dots \ \mathbf{h}_N]^T$ with $\mathbf{h}_n = [h_{n,1} \ h_{n,2} \ \dots \ h_{n,M}]^T$. The $N \times 1$ received signal \mathbf{y} is

$$\mathbf{y} = [y_1 \ y_2 \ \dots \ y_N]^T = \mathbf{H}\mathbf{W}\mathbf{x} + \mathbf{n} \quad (1)$$

where $\mathbf{x} = [x_1 \ x_2 \ \dots \ x_M]^T$ is the $M \times 1$ signal vector transmitted by the source with $\mathbf{R}_{\mathbf{x}} = \mathbb{E}\{\mathbf{x}\mathbf{x}^H\} = \frac{P}{M}\mathbf{I}_M$, P is the total transmit power, $\mathbf{W} = [\mathbf{w}_1 \ \mathbf{w}_2 \ \dots \ \mathbf{w}_M]$ is a $M \times M$ MIMO beamforming precoding matrix with $\|\mathbf{w}_m\|_2 = 1$, $\mathbf{n} \sim \mathcal{CN}(0, \sigma^2 \mathbf{I}_N)$ is a complex circular white Gaussian vector, $[\cdot]^T$ and $[\cdot]^H$ denotes the transpose operator and

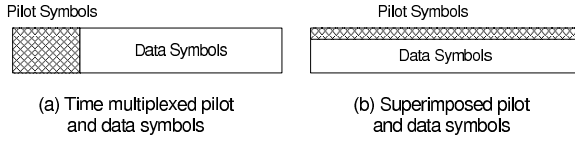


Fig. 1. Pilot patterns for channel estimation.

Hermitian conjugate operator, respectively. It is known that the spectral efficiency of MIMO flat-fading channel is

$$\eta = \log \left| \mathbf{I}_N + \frac{P}{M} \mathbf{H} \mathbf{W} \mathbf{W}^H \mathbf{H}^H \right| = \sum_{k=1}^K \log \left(1 + \frac{\rho_i}{M} \right) \quad (2)$$

where ρ_i denotes the received signal-to-noise ratio (SNR) of the k th beam, which is given by

$$\rho_i = \frac{\text{var}\{\mathbf{H} \mathbf{w}_i x_i\}}{\sigma^2} = \frac{\lambda_i P_i}{\sigma^2} \quad (3)$$

with λ_i denoting the i th eigenvalue of the MIMO channel autocorrelation matrix \mathbf{R}_H defined by

$$\mathbf{R}_H = \mathbf{H}^H \mathbf{H} = \sum_{m=1}^M \mathbf{h}_m \mathbf{h}_m^H = \sum_{i=1}^M \lambda_i \mathbf{v}_i \mathbf{v}_i^H, \quad (4)$$

\mathbf{v}_i denotes the i th eigenvector, the operator $|\cdot|$ denotes the determinant of matrix \cdot , and $\text{var}\{\cdot\}$ denotes the variance of random variable \cdot . (2) and (3) are the results from the assumption of perfect CSI available at transmitter. This may not be consistent with practical applications.

In reality, most MIMO receivers estimate \mathbf{H} or \mathbf{R}_H with the pilots sent by transmitter at first. Accuracy of the channel estimation depends on pilot design and placement. There are two popular pilot patterns, TMP and SIP, receiving much attention for MIMO channel estimation. They are shown in Fig. 1. TMP is a typical example of orthogonal pilot design where pilot symbols and data symbols are separated in time and/or frequency domain, which makes them orthogonal to each other. With orthogonal pilots, the channel estimation and data demodulation can be done separately which may lead to simple receiver design [7]. SIP does the opposite [8]. In SIP design, pilots and data nonorthogonally share the same time period and frequency band. In this case, joint channel estimation/demodulation and the demodulation with pilot interference cancellation are among the most popular receiver design techniques. After channel estimation, receiver will choose a beamforming vector from a shared MIMO precoding codebook. This is called channel quantization. And receiver then feeds back the chosen precoding index(es) to transmitter(s) instead of actual channel response for the next transmit precoding. With a MIMO codebook \mathcal{W} of the size 2^B consisting of M -dimensional normalized vectors $\{\mathbf{w}_1, \dots, \mathbf{w}_{2^B}\}$, it takes the receiver to feedback B bits for each beam stream. A codebook is usually designed to quantize channel responses with certain distortion measures [2]. This is related to Grassmannian line packing and the spherical packing on unit sphere $\mathcal{S}_n(1)$ [6], where $\mathcal{S}_n(R) = \{\mathbf{v} : \|\mathbf{v}\| = R\}$ denotes $(n-1)$ -sphere of radius R . When a codeword \mathbf{w}_k is chosen to precode transmit signals for i th beam \mathbf{v}_i at

the transmitter side, some degradation will usually happen on the signals received by receiver because of imperfect channel estimation and finite-rate feedback. This degradation on received signals can be expressed by

$$\delta_i = \min_{\mathbf{w} \in \mathcal{W}} \|\mathbf{H}(\mathbf{v}_i - \mathbf{w})\| = \lambda_i (1 - \mathbf{v}_i^H \mathbf{w}_k) - \sum_{j \neq i} \lambda_j \mathbf{v}_j^H \mathbf{w}_k \quad (5)$$

where \mathbf{v}_i is the ideal precoding vector for the i th eigen-mode. δ_i is known to be one of the major factors limiting closed-loop MIMO beamforming throughput. There are two components within δ_i . The first term is

$$\Delta = \lambda_i (1 - \mathbf{v}_i^H \mathbf{w}_k) = (1 - \alpha_i) \lambda_i, \quad (6)$$

which denotes the degradation of antenna gain with

$$\alpha_i = \mathbf{v}_i^H \mathbf{w}_k. \quad (7)$$

The second term is

$$I = \sum_{j \neq i} \lambda_j \mathbf{v}_j^H \mathbf{w}_k = \sum_{j \neq i} \alpha_j \lambda_j \quad (8)$$

denoting inter-beam interference (IBI) due to the correlation between \mathbf{w}_k and other eigen-modes $\{\mathbf{v}_j : j \neq i\}$. The average received SINR for the i th eigen-mode with the precoding codeword \mathbf{w}_k can be written by

$$\bar{\rho}_i = E_{\mathbf{v}_i \in \mathcal{V}_k} \left\{ \frac{\alpha_i^2 \rho_i}{1 + \lambda_i \sum_{l \neq i} \frac{\alpha_l^2}{\lambda_l} \rho_l} \right\} \quad (9)$$

with $K \leq \min\{M, N\}$ the spatial multiplexity order.

The achievable throughput of MIMO beamforming depends on not only the chosen precoding vectors $\{\mathbf{w}_k : k = 1, 2, \dots, K\}$ but also the power distribution $\{P_k : k = 1, 2, \dots, K\}$. There are many power allocation strategies for assigning transmit power to beams with different performance metrics. When maximizing throughput is a major concern, the so-called water-filling strategy can be an option, in which each beam's transmit power of each beam satisfies

$$P_k = \left(\mu - \frac{\sigma_n^2}{\lambda_k} \right)^+ = \begin{cases} \mu - \frac{\sigma_n^2}{\lambda_k} & \mu - \frac{\sigma_n^2}{\lambda_k} > 0 \\ 0 & \mu - \frac{\sigma_n^2}{\lambda_k} < 0 \end{cases} \quad (10)$$

with μ chosen so that the total power constraint is satisfied

$$\sum_{k=1}^K P_k = P. \quad (11)$$

If a delay-limited power allocation strategy is used, then

$$P_k = \frac{\mu}{\lambda_k} \quad (12)$$

with μ chosen to satisfy (11). It is also called channel inversion strategy. Another simple but popular strategy for allocating transmit power is to assign each beam the average power

$$P_k = \frac{P}{K}. \quad (13)$$

In the following sections, we will discuss how the channel quantization error and imperfect channel estimation affect MIMO beamforming and MIMO relay network.

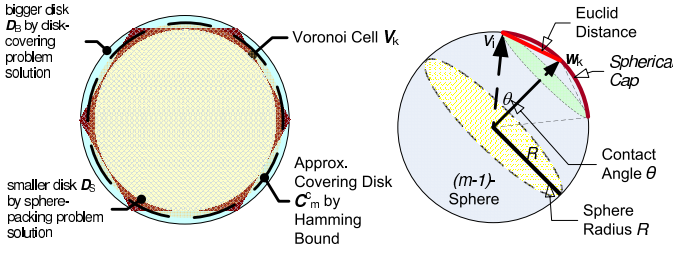


Fig. 2. (1) Voronoi cell and various bounds. (2) Sphere and sphere cap.

III. HAMMING BOUND ON CHANNEL QUANTIZATION

It is known that the performance of channel quantization depends on the codebook Voronoi decomposition. If the Voronoi decomposition is known, the statistic of the α_i defined in (7) and the $\bar{\rho}_i$ in (9) can be calculated. However, the closed-form expression of a general Voronoi cell boundary is an open-problem even for regular Voronoi tessellation. This makes it difficult to obtain some insights into the average SINR and achievable throughput for the MIMO beamforming with finite-rate feedback. There are two other well-known open problems related to Voronoi decomposition. The first one is called disk-covering problem in which, given a unit disk, the problem is to find the smallest radius for n equal disks to completely cover the unit disk. The other one is sphere-packing problem which concerns arrangements of non-overlapping identical spheres to fill a space. The relationship between Voronoi cell and the solutions to the disk-covering problem and sphere-packing problem is illustrated in Fig. 2. Basically the sphere-packing solution gives a lower-bound approximation of Voronoi cell and the disk-covering solution presents an upper-bound approximation of it. The difference is measured by the parameter called *packing efficiency*, which approaches 1 when the sphere dimension becomes large.

Instead of finding the exact boundary for the Voronoi cell V_i , we suggest a heuristic approach using Hamming bound and sphere cap to approximate the actual polytope boundary. It also is an approximate of the sphere packing solution, in which all spheres are supposed to be non-overlappedly placed. With our approach, sphere caps are overlapped with each other in space but the interior of them has the same area as the Voronoi cell. The border of this sphere cap is termed Hamming boundary. The relationship between Hamming boundary and Voronoi cell is shown in Fig. 2. For an uniform random codebook of size 2^B in M -dimensional Euclid space, the area of a Voronoi cell is given by

$$A(V_k) = \frac{2\pi^M}{2^B \Gamma(M)} \quad (14)$$

where $\Gamma(*)$ denotes the gamma function. On the other hand, the area of $(m-1)$ -complex sphere cap $C_m^c(\psi, R)$ with contact angle ψ and radius R is

$$A(C_m^c(\psi, R)) = [1 - \cos^{2(m-1)}(\psi)] S_m^c(R), \quad (15)$$

where $S_m^c(R)$ denotes a M -dimension complex ball in Euclid space with the radius R . The relationship between $S_m^c(R)$ and

$C_m^c(\psi, R)$ can be shown in Fig. 2 and it can be verified that

$$A(S_m^c(R)) = A(C_m^c(\pi, R)). \quad (16)$$

With matching the sum area of the sphere-cap with the whole sphere area, the boundary of a Voronoi cell can be approximated by a hypersphere or a closed space curve defined in the following proposition.

Proposition 1. (Hamming Boundary) *The boundary of the uniform complex Voronoi cell V_k can be approximated by a $(M-1)$ -unit complex sphere or a closed complex space curve.*

$$\begin{aligned} B(V_k) &\approx S_M^c(1) \cap \mathcal{L}_M^c(\mathbf{w}_k, \cos(\theta)) \\ &= \{\mathbf{v} : \|\mathbf{v}\| = 1, \angle(\mathbf{v}, \mathbf{w}_k) = \theta\}, \end{aligned} \quad (17)$$

where $\mathcal{L}_M^c(\mathbf{w}_k, \cos(\theta)) = \{\mathbf{v} : \mathbf{v}^H \mathbf{w}_k = \cos(\theta)\}$ denotes a complex space curve and θ is

$$\theta = \arccos(\alpha_0) \quad (18)$$

with

$$\alpha_0 = \left(\frac{2^B - 1}{2^B} \right)^{\frac{1}{2M-2}}. \quad (19)$$

On the other hand, if the ideal channel precoding vector \mathbf{v}_i is assumed to be a random variable of M -dimensional uniform distribution, the probability density function (PDF) $\text{pr}(\alpha)$ of α are

$$\begin{aligned} \text{pr}(\alpha) &= \text{Prob}\{x = \alpha\} \\ &= \begin{cases} 0 & 0 \leq \alpha < \alpha_0 \\ \frac{(2M-2)\alpha(1-\alpha^2)^{M-2}}{(1-\alpha_0^2)^{M-1}} & \alpha_0 \leq \alpha \leq 1 \end{cases} \end{aligned} \quad (20)$$

and the cumulated density function (CDF) is

$$\begin{aligned} \text{Pr}(\alpha) &= \text{Prob}\{x \leq \alpha\} \\ &= \begin{cases} 0 & 0 \leq \alpha < \alpha_0 \\ 1 - \left(\frac{1-\alpha^2}{1-\alpha_0^2} \right)^{M-1} & \alpha_0 \leq \alpha \leq 1 \end{cases}. \end{aligned} \quad (21)$$

With the assumption of uniform random codebook and MIMO channels, the average received SINR $\bar{\rho}_i$ can be approximated by the following lemma.

Lemma 1. *A heuristic mean of ρ_i can be expressed by*

$$\bar{\rho}_i \approx \frac{\sigma_\alpha^2 \rho_i}{1 + \left(\frac{1-\sigma_\alpha^2}{M-1} \right)^2 \sum_{j \neq i} \frac{\lambda_j}{\lambda_j} \rho_j}, \quad (22)$$

where σ_α denotes the standard deviation of α with

$$\sigma_\alpha^2 = E\{\alpha_i^2\} = \frac{1}{M} + \frac{M-1}{M} \left(\frac{2^B-1}{2^B} \right)^{\frac{1}{M-1}}. \quad (23)$$

IV. CRAMER-RAO BOUND ON CHANNEL ESTIMAT.

In previous discussions, neither inter-symbol interference (ISI) nor channel estimation was assumed. In general, the channel estimation model for frequency-selective block fading channel is different to (1). In practical channel estimation, not only the whole channel impulse response but also the pilot placement should be considered. Considering a M -input/ N -output MIMO channel with frequency-selective block fading, where the random channels taps remain constant for some data

packets and change to independent values for the next block, the received baseband signal can be written by

$$\mathbf{y} = \begin{bmatrix} y_1(t) & y_2(t) & \cdots & y_N(t) \end{bmatrix}^T$$

$$= \begin{bmatrix} \sum_{m=1}^M h_{m,1}(t) \otimes s_m(t) \\ \sum_{m=1}^M h_{m,2}(t) \otimes s_m(t) \\ \vdots \\ \sum_{m=1}^M h_{m,N}(t) \otimes s_m(t) \end{bmatrix} + \begin{bmatrix} n_1(t) \\ n_2(t) \\ \vdots \\ n_N(t) \end{bmatrix} = \mathbf{S}\mathbf{h} + \mathbf{n} \quad (24)$$

where $s_m(t)$ denotes the transmitted symbol from the m th antenna, \mathbf{h} is the stretched channel vector defined by

$$\mathbf{h} = \text{vec}([\text{vec}(\mathbf{H}_1) \text{vec}(\mathbf{H}_2) \dots \text{vec}(\mathbf{H}_N)]) \quad (25)$$

with $\mathbf{H}_n = [\mathbf{h}_n(0) \mathbf{h}_n(1) \dots \mathbf{h}_n(L_c - 1)]$, $\mathbf{h}_n(l) = [h_{n,1}(l) h_{n,2}(l) \dots h_{n,M}(l)]^T$ for $1 \leq l \leq L_c$, and

$$\mathbf{S} = \text{kron}([\mathbf{S}_1 \mathbf{S}_2 \dots \mathbf{S}_M]^T, \mathbf{I}) \quad (26)$$

with

$$\mathbf{S}_k = \begin{bmatrix} s_k(L) & \cdots & s_k(L - L_c) \\ s_k(L - 1) & \cdots & s_k(L - L_c - 1) \\ \vdots & \ddots & \vdots \\ s_k(1) & \cdots & s_k(1 - L_c) \end{bmatrix}. \quad (27)$$

L_c is the maximum channel order for all subchannels. After the channel response vector \mathbf{h} is estimated, we can calculate the channel correlation matrix \mathbf{R}_H by

$$\hat{\mathbf{R}}_H = \frac{1}{L_c} \sum_{l=1}^{L_c} \sum_{n=1}^N \hat{\mathbf{h}}_n(L_c + l) \hat{\mathbf{h}}_n^H(L_c + l). \quad (28)$$

There are many ways putting pilot symbols and data symbols together for PAT. We focus on two most popular designs: an orthogonal design by TMP pattern, and a non-orthogonal design by SIP pattern, in this paper.

1) *Time-Multiplexed Pilots and Data*: The concept of TMP design is to send Q known pilot symbols and $(L - Q)$ data symbols consecutively and separately in time domain. One possible example of TMP is shown in Fig. 1(a), in which the transmitted symbol $s_k(l)$ is

$$s_k(l) = \begin{cases} s_{pk}(l) & 1 \leq l \leq Q \\ s_{dk}(l - Q) & Q + 1 \leq l \leq L \end{cases}, \quad (29)$$

where $s_{pk}(t)$, $1 \leq t \leq Q$, denotes the pilot symbols transmitted in power σ_p^2 and $s_{dk}(t)$, $Q + 1 \leq t \leq L$, denotes the data symbols transmitted in power σ_d^2 .

2) *Superimposed Pilots and Data*: In SIP design, data symbols and pilot symbols are simultaneously sent within one frame of L symbols. This can be shown in Fig. 1(b). In this case, the transmitted symbol $s_k(l)$ becomes

$$s_k(l) = \frac{\sigma_p}{P} s_{pk}(l) + \frac{\sigma_d}{P} s_{dk}(l), \quad 1 \leq l \leq L, \quad (30)$$

with $\sigma_p^2 + \sigma_d^2 = P$.

The lower bound to the mean-squared errors (MSE) of unbiased channel estimates is given by CRLB, which is defined as the inverse of the Fisher Information Matrix (FIM). If we denotes $\boldsymbol{\vartheta} = [\mathbf{h}^T \mathbf{s}_d^T]^T$, the complex FIM is given by

$$\mathbf{F}(\boldsymbol{\vartheta}) = \mathbb{E} \left\{ \left[\frac{\partial \ln \Pr(\mathbf{y}|\boldsymbol{\vartheta})}{\partial \boldsymbol{\vartheta}^*} \right] \left[\frac{\partial \ln \Pr(\mathbf{y}|\boldsymbol{\vartheta})}{\partial \boldsymbol{\vartheta}^*} \right]^H \right\}. \quad (31)$$

With (31), the MSE of the estimates of $\mathbf{R}_h = \mathbb{E} \{\mathbf{h}\mathbf{h}^H\}$ is given by

$$\text{MSE} \{\mathbf{R}_h\} = \sigma_n^2 [\mathbb{E} \{\mathbf{S}^H \mathbf{S}\} + \rho_h^2 \mathbf{I}]^{-1}, \quad (32)$$

where $\rho_h^2 = \mathbb{E} \left\{ \left| \frac{\partial \ln \Pr(h)}{\partial h^*} \right|^2 \right\}$. The CRLB on the channel estimation therefore is formulated by the following lemma.

Lemma 2. (Cramer-Rao Lower Bound) For the time-multiplexed pilot and data design defined in (29), the CRLB of channel estimation is

$$\varepsilon_h^{\text{TMP}} \geq [\rho_h^2 + Q\rho_p^2 + (L - Q)\rho_d^2]^{-1}. \quad (33)$$

For the superimposed pilot and data design defined in (30), the CRLB of channel estimation is

$$\varepsilon_h^{\text{SIP}} \geq [\rho_h^2 + L(\rho_p^2 + \rho_d^2)]^{-1} \quad (34)$$

where $\rho_p^2 = \frac{\sigma_p^2}{\sigma_n^2}$ denotes the SNR of received pilot signals and $\rho_d^2 = \frac{\sigma_d^2}{\sigma_n^2}$ denotes the SNR of received data signals.

Now if we look back at (28) with the assumption that the channel is constant during estimation, pilots and data are random and independent to each and an optimal channel estimation is done by receiver, a heuristic view of the MIMO channel correlation matrix \mathbf{R}_H estimation is

$$\Delta_{\mathbf{R}_H} = \hat{\mathbf{R}}_H - \mathbf{R}_H \approx \frac{\varepsilon_h}{\sqrt{L_c N}} \mathbf{I}_M. \quad (35)$$

The eigenvalue estimation error can be approximated by

$$\Delta_{\lambda_k} \approx \mathbf{v}_k^H \Delta_{\mathbf{R}_H} \mathbf{v}_k - \lambda_k \left(\Delta_{\mathbf{v}_k}^H \mathbf{v}_k + \mathbf{v}_k^H \Delta_{\mathbf{v}_k} \right) \quad (36)$$

where ε_h denotes the MSE of channel estimates, which can be either $\varepsilon_h^{\text{TMP}}$ or $\varepsilon_h^{\text{SIP}}$. With (35) and (36), it shows that $\Delta_{\mathbf{R}_H}$ mostly affects the accuracy of the eigenvalues estimates $\{\hat{\lambda}_k, k = 1, 2, \dots, K\}$ if enough pilots are available. The MSE of eigenvalue estimates is roughly bounded by

$$\varepsilon_{\lambda} \gtrsim \frac{\varepsilon_h}{\sqrt{L_c N}}. \quad (37)$$

There are two major effects of PAT on MIMO channel throughput. The first one is that pilot itself will take away channel resources from data transmission. The second one is that it may affect the transmit power allocation. If orthogonal pilot pattern is used, there will be linearly degradation on channel throughput so that

$$\eta^{\text{TMP}} = \frac{L-Q}{L} \sum_{k=1}^K \log \left(1 + \frac{\hat{\rho}_i}{M} \right), \quad (38)$$

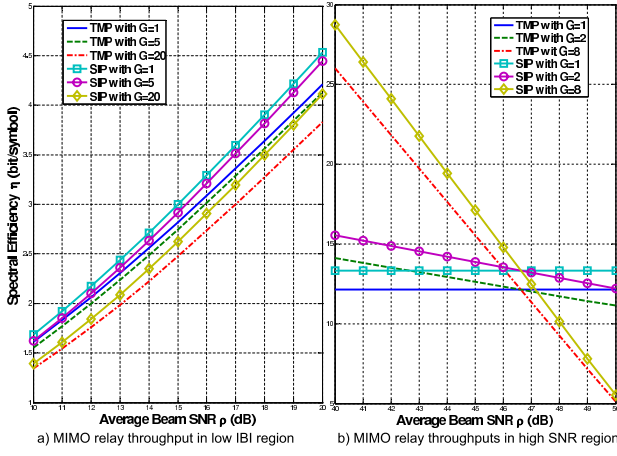


Fig. 3. MIMO relay throughput with $M = N = B = 4$ and $\frac{Q}{L} = \frac{\sigma_d^2}{P} = 10\%$.

where $\hat{\rho}_i$ denotes the suboptimal power allocation due to channel estimation error, and if superimposed pilot pattern is employed, the throughput becomes

$$\eta^{\text{SIP}} = \sum_{k=1}^K \log \left(1 + \frac{\sigma_d^2 \hat{\rho}_i}{P} \right), \quad (39)$$

even though the ideal beamforming vectors $\{\mathbf{v}_k : k = 1, 2, \dots, K\}$ are available.

V. MULTI-ANTENNA RELAY NETWORK

In order to understand the asymptotic behavior of MIMO beamforming with channel estimation and quantization, a multi-hop MIMO relay network with amplify-and-forward (AF) transmission in each relay station is considered. With previous discussions, the follow conclusion can be reached.

Lemma 3. *In an AF MIMO relay network where each relay station has a $M \times N$ MIMO transceiver with spatial multiplexity order K and each MIMO link with same pilot pattern and codebook is independent random, the end-to-end average throughput for MIMO relay link of the size G is*

$$\bar{\eta}^{\text{TMP}} \approx \frac{L-Q}{L} K \log \left[1 + \frac{\rho}{M} \left(\frac{\sigma_\alpha^2}{1 + \frac{(K-1)(1-\sigma_\alpha)^2 \rho}{(M-1)^2}} \right)^G \right] \quad (40)$$

if time-multiplexed pilot pattern is used, or

$$\bar{\eta}^{\text{SIP}} \approx K \log \left[1 + \frac{\sigma_d^2 \rho}{PM} \left(\frac{\sigma_\alpha^2}{1 + \frac{(K-1)(1-\sigma_\alpha)^2 \rho}{(M-1)^2}} \right)^G \right] \quad (41)$$

if superimposed pilot pattern is used, where $\rho = E\{\rho_k\}$ denotes the average received beamforming SNR and σ_α^2 is defined in (23).

If the performance of multi-antenna relay network with MISO or neglectable IBI is considered, the end-to-end throughput with TMP becomes

$$\bar{\eta}^{\text{TMP}} \approx \frac{(L-Q)K}{L} \log \left[1 + \frac{\sigma_\alpha^2 \rho}{M} \right] \quad (42)$$

and the end-to-end throughput with SIP is

$$\bar{\eta}^{\text{SIP}} \approx K \log \left[1 + \frac{\sigma_d^2 \sigma_\alpha^2 \rho}{PM} \right]. \quad (43)$$

They basically are the same as direct MIMO with additional relay channel degradation factor σ_α^2 . An example of MIMO relay throughput is shown in Fig. 3(a). It shows that SIP is outperform TMP and the end-to-end throughput of both cases decreases with more hops. Therefore it may be more efficient to increase SNR instead of use more hops to increase network throughput. If the performance of multi-antenna relay network in high SNR region is concerned, (40) is

$$\bar{\eta}^{\text{TMP}} \approx \frac{(L-Q)K}{L} \log \left[1 + \frac{(M-1)^G}{M \rho^{G-1}} \left(\frac{\sigma_\alpha}{1-\sigma_\alpha} \right)^{2G} \right] \quad (44)$$

and (41) becomes

$$\bar{\eta}^{\text{SIP}} \approx K \log \left[1 + \frac{\sigma_d^2}{P} \frac{(M-1)^G}{M \rho^{G-1}} \left(\frac{\sigma_\alpha}{1-\sigma_\alpha} \right)^{2G} \right]. \quad (45)$$

With (44) and (45), it shows that the end-to-end throughput of MIMO relay network with channel estimation and quantization actually will decrease in high SNR region even though the transmit power of each hop increases. This can be shown by Fig. 3(b), where higher SNR actually brings down the network throughput and therefore it may be more efficient to use more hops instead of increase SNR in each hop to increase network throughput. This means that the network capacity becomes interference-limited. This is different to the low-IBI case.

VI. CONCLUSIONS

In this paper, a Hamming boundary for codebook Voronoi decomposition and the beamforming SINR with finite-rate feedback are formulated. And the effects of imperfect channel estimation with time-multiplexed pilot pattern or superimposed pilot pattern on MIMO beamforming are discussed. Finally the scalability and the tradeoffs in increasing MIMO relay network throughput with imperfect channel estimation and quantization are discussed.

REFERENCES

- [1] D. Gerlach and A. Paulraj. Spectrum reuse using transmitting antenna arrays with feedback. In *Proc. Int. Conf. Acoust., Speech, Signal Processing*, pages 97–100, Adelaide, Australia, April 1994.
- [2] A. Narula, et al. Efficient use of side information in multiple-antenna data transmission over fading channels. *IEEE J. Select Areas in Communications*, 16(8):1423–1436, October 1998.
- [3] K. K. Mukkavilli, A. Sabharwal, E. Erkip and B. Aazhang. On beamforming with finite rate feedback in multiple-antenna systems. *IEEE Trans Info. Theo.*, 49:2562–2579, October 2003.
- [4] P. Xia and G. B. Giannakis. Design and analysis of transmit-beamforming based on limited-rate feedback. In *Proc. IEEE VTC*, September 2004.
- [5] J. C. Roh and B. D. Rao. Performance analysis of multiple antenna systems with vq-based feedback. In *Proc. Asilomar Conference 2004*, Pacific Grove, CA, November 2004.
- [6] D. J. Love, R. W. Heath and T. Strohmer. Quantized maximal ratio transmission for multiple-input multiple-output wireless systems. In *Proc. Asilomar Conf.*, Pacific Grove, CA, Nov. 2002.
- [7] L. Tong, B. M. Sadler and M. Dong. Pilot-assisted wireless transmissions: general model, design criteria, and signal processing. *IEEE Signal Processing Mag.*, 21(56):12–25, November 2004.
- [8] M. Coldrey and P. Bohlin. Training-based mimo syetems: Part ii. *Technical Report (http://db.s2.chalmers.se/)*, (R032/033), June 2006.